Contaminant Transport in Groundwater, Kobus & Kinzelbach (eds)
 ISBN 90 6191 879 0

Mass transport in an artificial heterogeneous aquifer: Experiments and numerical modelling

G.Schäfer & H.E.Kobus
Institut für Wasserbau, Universität Stuttgart, FR Germany

ABSTRACT: In order to generate a data base for the numerical study of dispersion processes in a well defined heterogeneous porous medium, a laboratory tank of 14 m in length, 0.5 m in height and 0.13 m in width has been constructed, which is composed of 81 different elements of exactly known geometry and hydraulic properties. In dispersion experiments using salt as tracer, breakthrough curves are observed at 80 points in 8 vertical sections. A comparison of three types of numerical models with the experimental data shows how well the models of various complexity describe the advection and dispersion processes and how in these cases the various dispersion parameters depend upon the models used.

1 INTRODUCTION

Mass transport in groundwater is strongly determined by the heterogeneities of the aquifer. In depth-averaged models, the disregarded vertical velocity variation results in an increase of disperision coefficients with the transport scale (Mercado, 1967; Gelhar and Axness, 1983). A more detailed modelling approach would require detailed information about the aquifer structure, which is usually not available.

A systematical experimental investigation in a large scale model aquifer has been carried out in order to generate a detailed data base for numerical studies. In dispersion experiments, the observed breakthrough curves reflect the transport behaviour due to the heterogeneous aquifer structure. The effects of permeability differences upon the longitudinal spreading have been studied using a continuous injection of tracer as well as a pulse injection.

The main objective of this paper is to outline the experimental studies performed in the artificial heterogeneous aquifer and to describe the mass transport with different types of numerical models. While the transport modelling with a 2D finite difference model contains the aquifer structure in all its known details, a simplified modelling approach using a two-layer model takes into account only characteristic parts of the aquifer. Further, the performance of the classical one-dimensional advection-dispersion equation, as the simplest approach for the interpretation of transport processes, is checked against the available experimental data.

2 PHYSICAL MODEL AND AQUIFER

The laboratory model consists of a steel flume with a transparent frontage having internal dimensions of 14 m x 0.5 m x 0.13 m (figure 1).

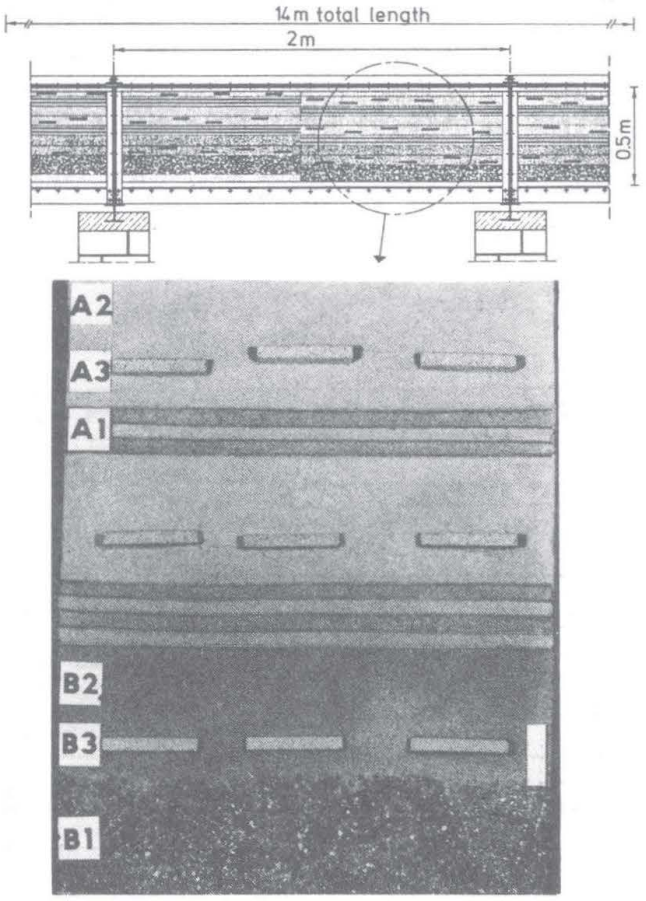

Fig.1 Physical model

All measurement devices are mounted at the backwall of the tank in 8 vertical sections at distances of 0.5, 1.25, 3.75, 4.5, 5.25, 8.75, 10.25 and 13.5 m from the inlet section (figure 2).

The inlet and outlet of the flume are screened over the entire cross-section. In order to avoid chanelling on the top part of the sands, a silicon film was pressed into the sands by a constantly applied pressure. Exactly controlled piezometric head boundaries at both ends of the model guarantee a constant discharge through the aquifer. The hydraulic gradient can be varied over a range from 3 to 13 percent.

The flume was packed using six model layers in order to construct a layered system with abrupt discontinuities of individual layers in the manner shown in figure 2. The experimental setup was designed by making numerical studies using a vertically 2D transport model (Schäfer,1987). Layer A is a heterogeneous region composed of individual layers A1, A2 and A3; layer B is more permeable than A, but similarly made up of three layers B1, B2 and B3 (see figure 2). The averaged hydraulic conductivity of layer B is about seven times higher than the one of layer A. The arrangements were made such that the depth-averaged permeability is constant, over the entire model aquifer.

In order to built up model layers with different hydraulic properties, three silicate sands and two types of porous ceramic plates were used. Sand 1 and 2 are uniform homogeneous sands with a mean grain size of 0.00038 and 0.00057m; sand 3 is a nonuniform heterogeneous sand with a mean grain size of 0.0015 m. The components of sand 3 are three uniform sands with mean grain sizes of 0.00057, 0.0015 and 0.0025 m and volume ratios of 40, 25 and 35 percent. The Darcy coefficients of the used sands were experimentally determined to be $2.8 \cdot 10^{-4}$ m/s (sand 1), $1.6 \cdot 10^{-3}$ m/s (sand 2) and $4.8 \cdot 10^{-3}$ m/s (sand 3). In order to represent randomly distributed heterogeneities, low- and high-permeability ceramic plates (0.08 x 0.01 x 0.05 m) with Darcy coefficients of $8 \cdot 10^{-5}$ m/s respectively $5 \cdot 10^{-4}$ m/s were used. The local dispersivities range from 0.0006 m (sand 1) to 0.0024 m (sand 3). These values confirm the functional relationship between mean grain size and dispersivity of the solid matrix (Pfannkuch,1963).

While layer A2 and B2 are built up with homogeneous silicate sand 1 and 2, layers A3 and B3 are mixtures of sands 2 and 3, respectively, and randomly distributed porous ceramic plates. In the case of layer A3 the permeability of the inclusions is about two times higher than that of the surrounding sand. Layer B3, however, includes ceramic plates with a lower permeability of only 5 percent compared to silicate sand 2. In both cases the pore volume of the ceramic plates per total pore volume is approximately 13 percent. Layer A1 is a composition of fine layers of high permeabiltiy (silicate sand 2) and low permeability (silicate sand 1). As to layer B1, it contains only silicate sand 3. The permeability, porosity and dispersivity of each model layer was tested in separate test series (Schäfer, 1987).

In order to study the transport behaviour in the given aquifer, both continuous and pulse injections of tracer over the entire cross-section at the model inlet as well as instantaneous point injections at several locations in the aquifer were performed. In this paper, the results of the cross-sectional tracer injection tests will be described.

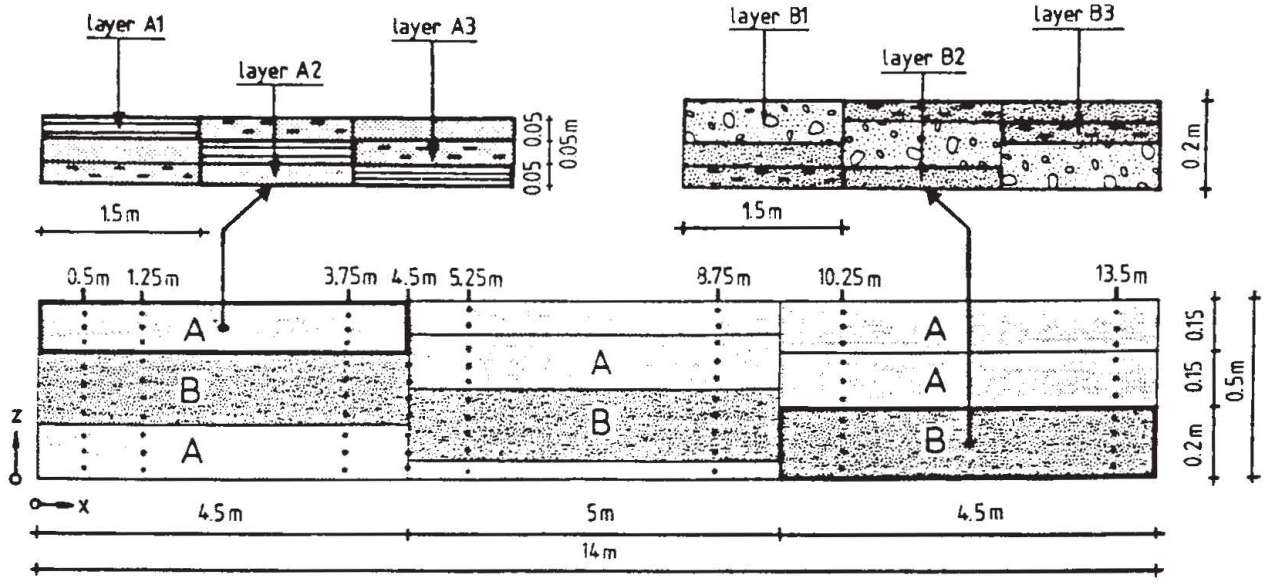

Fig.2 Aquifer structure

3 EXPERIMENTAL RESULTS

The dispersion experiments were performed using salt of low concentration (C_0<1 g/l) as a tracer labelled by a dye (uranin). The tracer of given concentration as well as the clean water was applied from a constant head tank. Each reservoir can be switched separately to the flume inlet chamber, which is equipped with valves and flushing ports for forced mixing in the inlet chamber. By suitable operation of the various valves and flushing ports, it was ensured that the tracer was introduced uniformly over the flume entrance cross section.

The experiments were conducted at a constant temperature of 20 °C. The concentration measurements were performed automatically at the conductivity cells in the aquifer and at one cell directly at the model outlet chamber.

Results of a continuous-injection tracer experiment are shown in figure 3. The normalized breakthrough curves given in the figure are measured 1.25 meters from the inlet at different elevations (see figure 2).

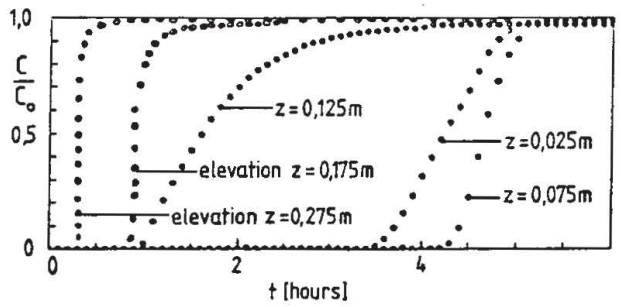

Fig.3 Measured breakthrough curves at a travel distance of 1.25 m at different elevations

Up to a travel distance of approximately 1.5 meters the streamlines are horizontal and hence mass transport can be studied separately in each homogeneous layer (see figure 3):

- elevations z = 0.075 m and z = 0.025 m (layer A2/A3): The breakthrough curve at the elevation of 0.075 m (layer A2) shows in comparison with the measurement at elevation of 0.025 m (layer A3) a steeper increase of concentration. The equivalent longitudinal dispersivity of layer A3 grows to several times of the dispersivity of the homogeneous layer A2. The results of experimental studies in porous media with local heterogeneities carried out by Herr et al., 1988, confirm this effect.
- elevation z = 0.125 m (layer A1): The transition zone at this elevation is the largest one. Due to the transverse exchange between fine layers of high and low permeability, the mass exchange causes a strong concentration tailing.
- elevation z = 0.175 m (layer B3): The breakthrough curve at this elevation shows that the mass transport in layer B3 is strongly determined by the effect of two transport regimes. The steep concentration increase is similar to the breakthrough curve observed in layer B2 and hence shows the influence of the silicate sand 2. The ceramic plates with a permeability less than the corresponding value of the surrounding sand, however, cause a concentration tailing. Such differences in transport behaviour in heterogeneous aquifers are also described in the experimental studies of Herr et al.,1988 and theoretically by Spitz, 1985.
- elevation z = 0.275 m (layer B1): The heterogeneous silicate sand 3 included in layer B1 has the highest permeability of all used sands. This causes the shortest tracer arrival time.

With increasing travel distance, the influence of the vertical velocity components on the tracer spreading becomes more and more evident. This can be seen from the measurements shown in figure 4 as well as in the photographs in figure 5.

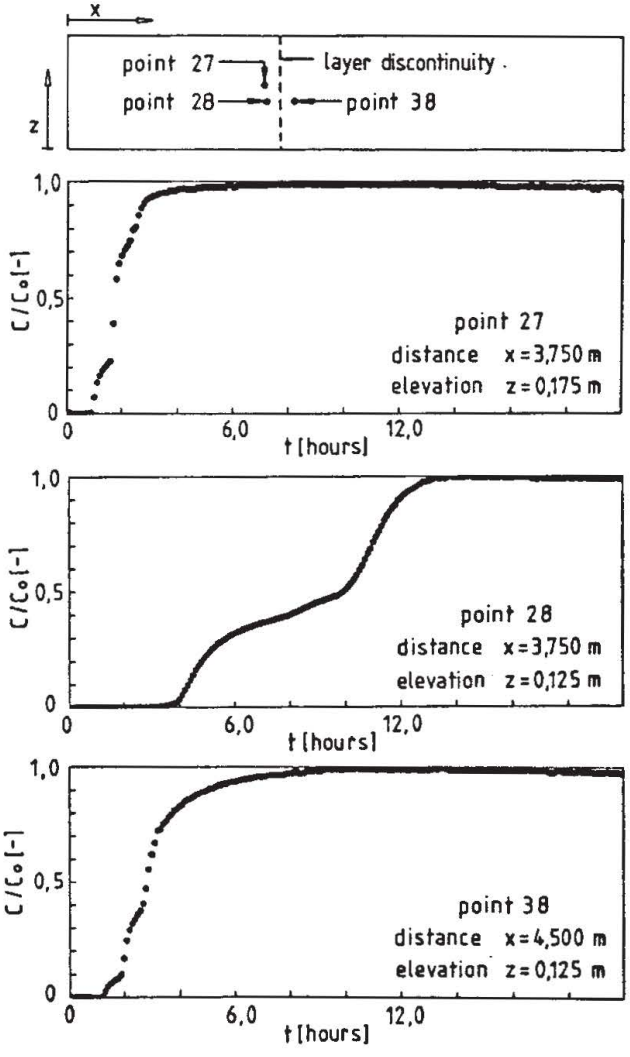

Fig.4 Observed breakthrough curves at distances of 3.75 m and 4.50 m

The breakthrough curve at measurement point

38, which is located 0.75 m downstream of measurement point 28 shows a markedly different behaviour (figure 4). The given change in the vertical sequence of model layers at the layer discontinuity causes a flow field with downward velocity components (see figure 5). Therefore the observed breakthrough curve at observation point 38 exhibits nearly the same shape as the breakthrough curve at observation point 27 which is located 0.05 m higher than point 28.

A second type of tracer experiment using a pulse injection was performed. The injection volume of the tracer pulse was equal to 10 per cent of the aquifer pore volume. This corresponds for the chosen hydraulic gradient to a pulse injection time of one hour. An illustration of the tracer spreading at a layer discontinuity is given in figure 5 with four photographs taken at different time intervals. The dominant role of the highly permeable layer (B1) is shown in the first photograph. With increasing time the tracer also arrives in the neighbouring low permeable layers at this cross-section, whereas in layer B1 the tracer pulse has already passed.

Figure 6 shows breakthrough curves at a distance of 10.25 m at different elevations (see figure 2). As discussed before, the tracer spreading is strongly influenced by the vertical two-dimensional flow field and hence depends on the hydraulic properties of different model layers. This can also be seen by the comparison of the

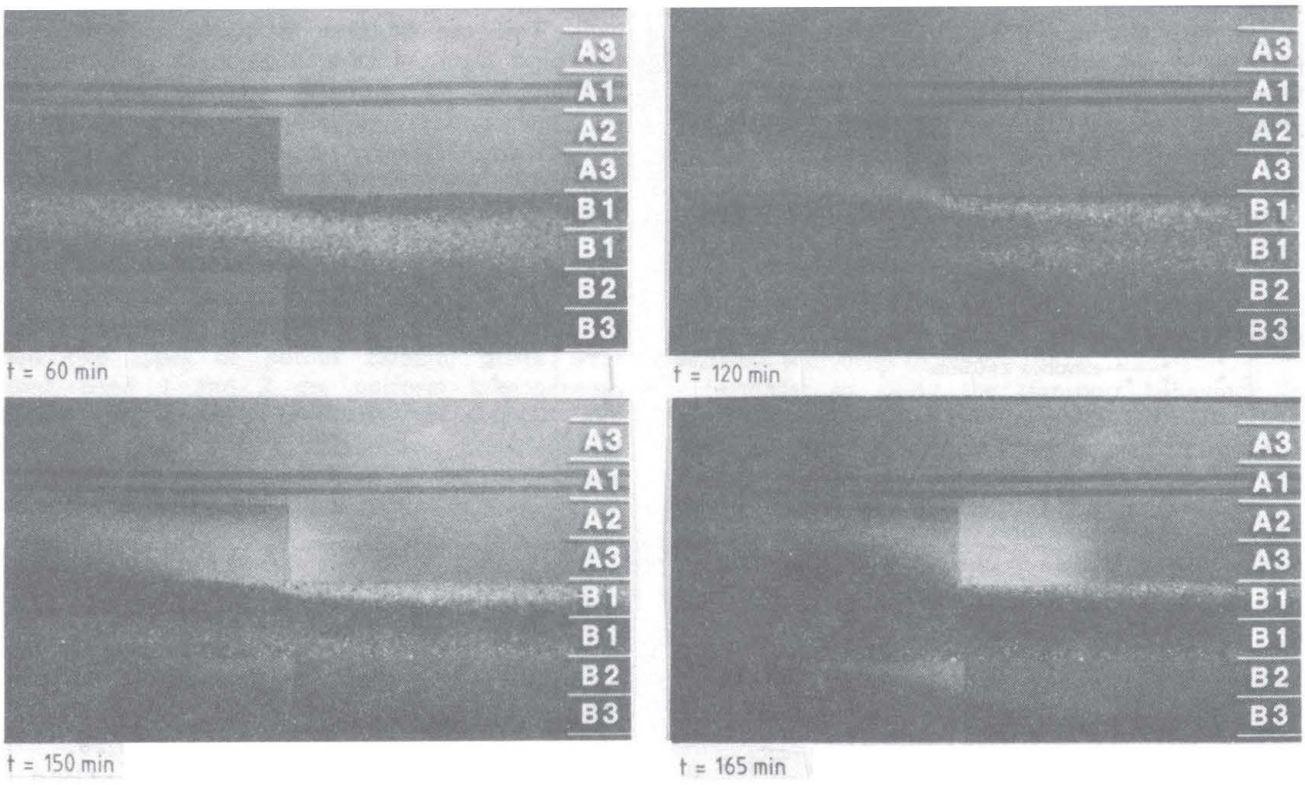

Fig.5 Pulse injection: Tracer spreading at a layer discontinuity (distance x = 4.50 m)

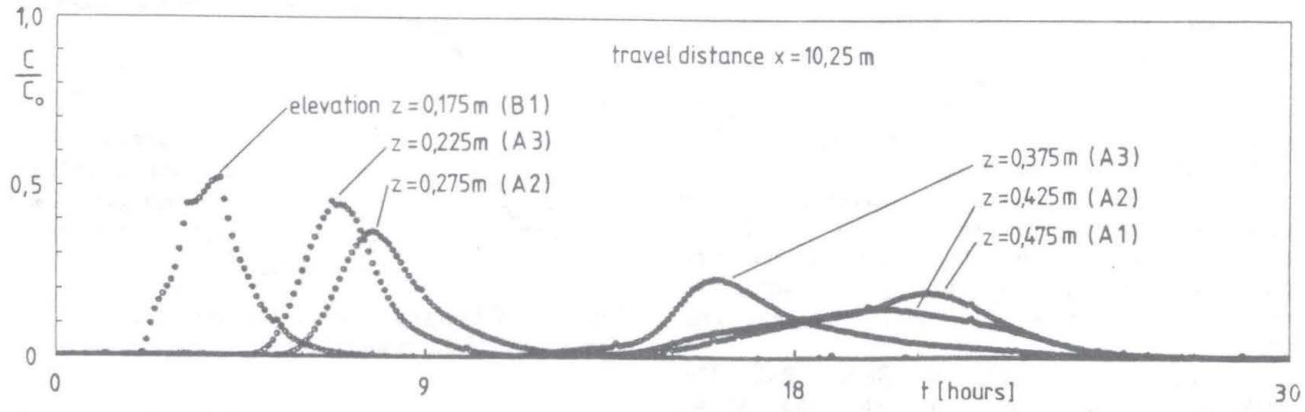

Fig.6 Pulse injection: Observed breakthrough curves at a travel distance of 10.25 m

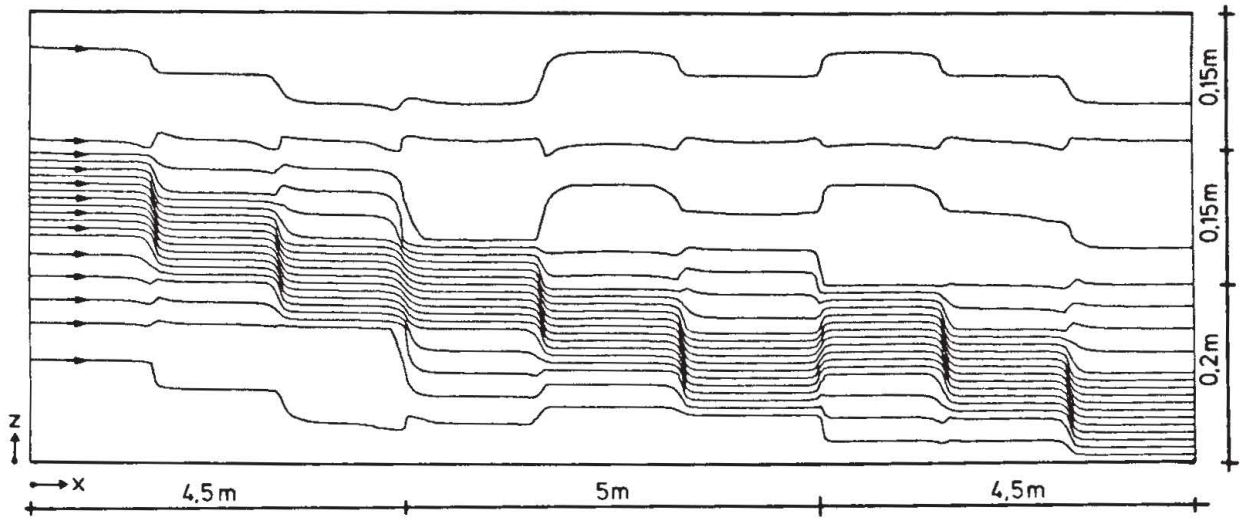

Fig.7 Computed streamline distribution

observed breakthrough curves at elevations z = 0.225 m and z = 0.375 m. The centre of mass arrives approximately twice as fast at elevation z = 0.225 m (layer A3) as in the higher located layer A3. Due to the vertical mass transport, the average pore velocities in the highly permeable layers (B1, B2, B3) decrease with travel length, while the average pore velocities in the low permeable layers (A1, A2, A3) increase.

4 VALIDATION OF A 2D TRANSPORT MODEL

The availability of the detailed information about the heterogeneous structure of the artificial aquifer allows detailed transport modelling using a vertically two-dimensional model.

The advection-dispersion equation is solved in the numerical model using centered (Crank-Nicolson) and implicit difference formulations in time. In order to keep numerical dispersion low, a space discretization of 0.01 m in length and height was chosen, which results in a total number of 72800 nodes. In the numerical model itself the longitudinal dispersivity was set equal to zero, because the numerical dispersivity is in the same order of magnitude as the physical dispersivity. The transverse dispersivity was chosen from the results of previous studies as ($\alpha_T = 0.05 \cdot 10^{-3}$ m). The application of the Crank-Nicolson scheme requires a Courant number less than one for the time step in order to avoid numerical instabilities. This restriction, together with the large number of nodes, required a powerful computer in mass storage as well as calculation speed (Cray 2).

The numerical model takes into account the detailed structure of the aquifer with all its known hydraulic properties. The Darcy coefficients of the used model layers range from $4.8 \cdot 10^{-3}$ m/s (layer B1) to $2.8 \cdot 10^{-4}$ m/s (layer A2); the measured porosities are about 38 percent. A detailed description of the hydraulic data is given in Schäfer, 1987. Figure 7 shows the calculated velocity field in the form of stream lines. The hydraulic properties of the model layers known from separate test series and the flow rate condition for a selected continuous-injection tracer experiment were used as input data. The streamlines illustrate the characteristic flow pattern of the artificial aquifer. Between layer discontinuities, streamlines are essentially horizontal and the flow rate in each layer depends on the given permeability. Near layer discontinuities the flow field exhibits vertical velocity components which cause a spreading and focussing, repectively, of the streamlines.

For constant flow conditions, mass transport was calculated for a tracer experiment with continuous injection at the inlet. The comparison with experimental results is shown for several observation points in figures 8 and 9.

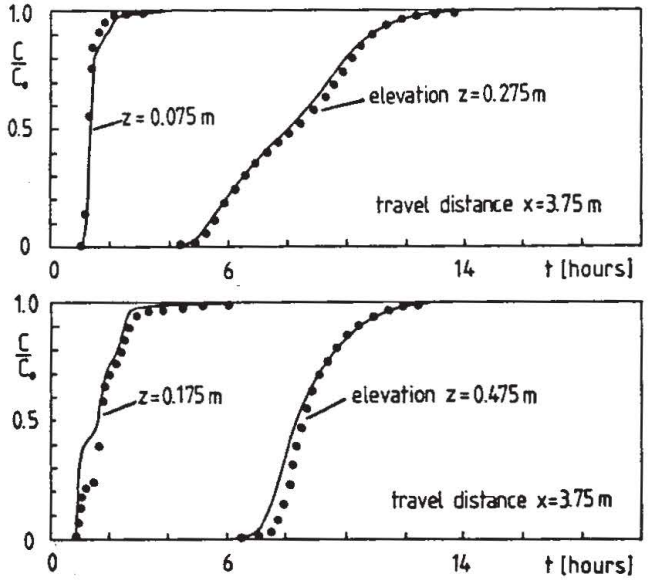

Fig.8 Measured (symbols) and computed (lines) breakthrough curves at a distance of x=3.75 m at different elevations

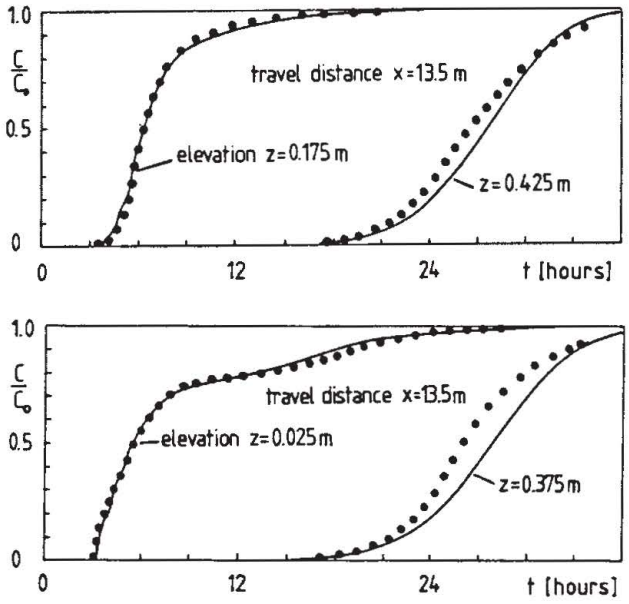

Fig.9 Measured (symbols) and computed (lines) breakthrough curves at a distance of x=13.5 m at different elevations

The calculated breakthrough curves fit well with the observed values. This shows that the transport processes in the model aquifer are well represented by the two-dimensional numerical model.

The good agreement of the numerical transport model with the experiment is underlined by figure 10, in which the calculated and measured breakthrough curves at the model outlet chamber are compared.

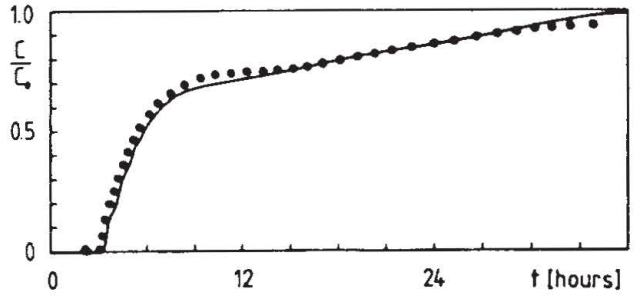

Fig.10 Comparison of calculated (line) and observed (symbols) breakthrough curves at the model outlet chamber

5 SIMPLIFIED MODELLING APPROACHES

Detailed modelling of the transport process needs large amounts of computer calculation time and mass storage and requires also detailed information about the aquifer structure. In order to reduce the requirements for the calculation procedure and the data base, two simplified modelling concepts are considered.

The simplest approach contains the classical one-dimensional (depth-averaged) advection-dispersion equation. The advection term, expressed by the average pore velocity, is chosen as the mean value (depth-averaged) of the model layers. The longitudinal dispersion coefficient is described by the product of the chosen average pore velocity and the mean value of the local dispersivities; the additional transition zone due to the vertical velocity variation is not taken into account. Results of a transport modelling with this simplified concept are shown later (see figure 13). Both parameters describe the tracer spreading accurately only when the asymptotic regime of the transport process is reached. As the tracer experiments with continous injection at the model inlet show, the measured breakthrough curves at the outlet chamber contain a steep concentration increase and a long concentration tailing. Therefore, the mass transport in the model aquifer can not be described by the classical one-dimensional concept.

A more datailed modelling approach is to use a two-layer model, in which the aquifer is composed of two regions of different mobility, each representing a characteristic part of the aquifer (figure 11).

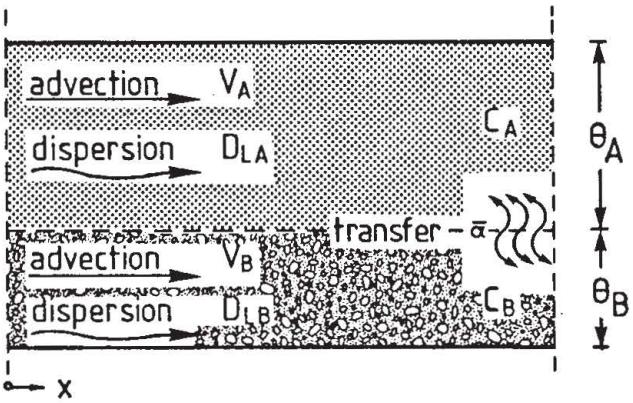

Fig.11 Two-layer model

The transport in each region is described by the one-dimensional advection-dispersion equation, with a transfer condition along the interface coupling the two layers. It is assumed that complete mixing occurs in both layers and that the mass flux between the two layers is proportional to the difference in concentrations (Skopp et al., 1981). The concentration in both layers can then be expressed by the transport equation as

$$\theta_A \frac{\partial c_A}{\partial t} + \bar{\alpha}(c_A - c_B) = \theta_A D_{LA} \frac{\partial^2 c_A}{\partial x^2} - \theta_A v_A \frac{\partial c_A}{\partial x} \quad (1)$$

$$\theta_B \frac{\partial c_B}{\partial t} + \bar{\alpha}(c_B - c_A) = \theta_B D_{LB} \frac{\partial^2 c_B}{\partial x^2} - \theta_B v_B \frac{\partial c_B}{\partial x} \quad (2)$$

where C_A and C_B are the concentrations of a noninteractive solute (kg/m^3) in layer A and B, V_A and V_B are the average pore velocities (in m/d), D_{LA} and D_{LB} are the longitudinal dispersion coefficients (in m^2/d), Θ_A and Θ_B are the water contents in these zones and $\bar{\alpha}$ is the mass transfer coefficient (in day^{-1}). Equation (1) and (2) are solved numerically by a finite difference scheme.

The average pore velocities V_A and V_B are chosen as the mean values of layer A (made up of A1, A2, A3) and layer B (made up of B1, B2, B3) near the model inlet. As a first approach, the dispersion coefficients D_{LA} and D_{LB} are put equal to the respective averaged local values, Θ_A and Θ_B are equal to the pore volume of layer A and layer B. The way how the mass transfer coefficient $\bar{\alpha}$ has been chosen will be described in the following two sections.

In parts of the aquifer where the streamlines are horizontal, the mass transfer normal to the streamlines is caused purely by lateral dispersion. Assuming that the mixing zone at the interface between two neighbouring streamlines is small compared with the thickness of the layers, the mass flux over the interface can be calculated using an analytical solution described by Shamir and Harleman, 1966. A comparison of this value with the mass transfer term used in the two-layer model gives the magnitude of the mass transfer coefficient.

A more significant vertical mass transfer takes place near layer discontinuities. Interrupted layers and vertical changes in hydraulic permeabilities cause an increase of vertical mixing (figure 12). Due to the layer discontinuities, the streamlines are spreading respectively focussing. As figure 12 shows, parts of the mass concentrated in layer B are transported into layer A. Assuming that the initial concentration in layer A is zero, the mass transfer coefficient $\bar{\alpha}$ can be estimated by a comparison of the mass flux M_{B-A} and the mass transfer introduced in the two-layer model. Applied to the flow field in the model aquifer, the mass transfer coefficents have been calculated in such a way at distances of 4.5, 6.1 and 9.5 m from the model inlet.

A numerical solution of equation (1) and (2) has been obtained, which takes into account the described hydraulic properties as well as the estimated magnitudes of the mass transfer coefficient. With this simplified model concept, depth-averaged breakthrough curves were calculated at different locations and compared with the numerical results of the two-dimensional transport model (figure 13).

Figure 13 shows that the results of the two-layer model describe the main features of the given breakthrough curves (results of the 2D transport model) much better than the depth-averaged model. Yet, they still exhibit some deviations from the results of the 2D transport

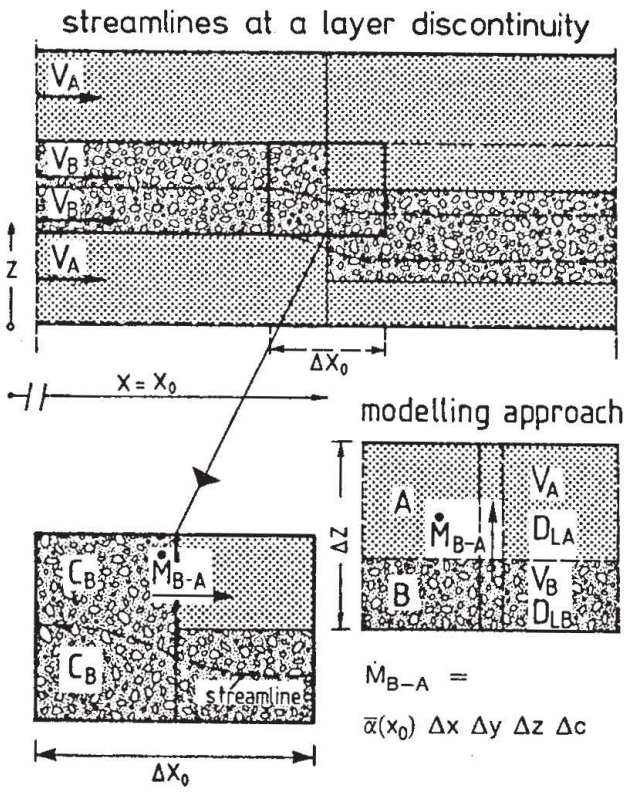

Fig.12 Estimation of the mass transfer coefficient

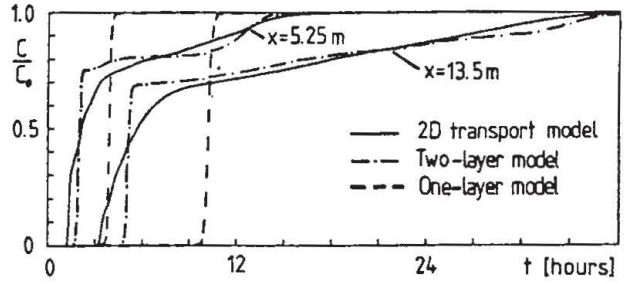

Fig.13 Comparison of depth-averaged breakthrough curves of the 2D transport model, the two-layer model and the one-layer model

model. The observed tailing is fairly well described for both travel distances with decreasing deviations at larger distances. However, the steep slope of both curves (distance x=5.25 m and x=13.5 m) does not fit well. This shows, that the assumed dispersion coefficients, identified as average local dispersion coefficients, do not represent the transition zone in the individual layers.

A similar result illustrates figure 14 by a comparison of calculated and measured breakthrough curves at the model outlet chamber. While the tailing in the breakthrough curves can be well described by the two-layer model, significant differences occur in the steep slope

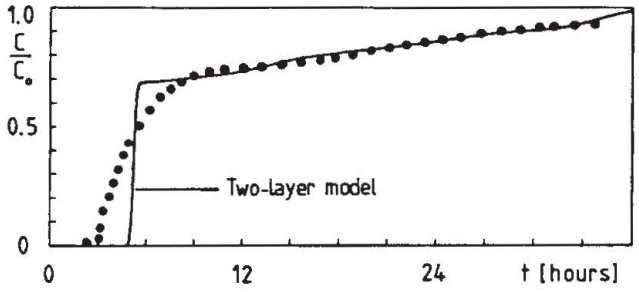

Fig.14 Comparison of calculated (line) and measured (symbols) breakthrough curves at the model outlet chamber

of the curves. In order to get a better approximation, the dispersion coefficients of layer A and B should take into account the increased values caused by the averaging process. This will be part of further research work.

6 CONCLUSIONS

The experimental investigations show that vertical mixing due to transverse dispersion is negligeably small compared with the effects of layer discontinuities in the aquifer structure. Application of a high resolution numerical model in two dimensions (vertical section) to the model aquifer showed that a good prediction of the transport processes is possible if all details of the aquifer structure are known. In this case, dispersion effects are small and can be identified with the transition zone due to the dispersivities at the local scale. Since the model aquifer exhibits two characteristic populations of markedly different properties, transport processes can not be described adequately by one-dimensional depth-averaged models. More promising are two-layer models which take into account at least two different velocity regimes coupled with a mass transfer condition along the interface. With reference to the mass flux normal to the layers, it was shown that the magnitude of the transfer coefficient introduced in this model can be estimated from the given aquifer structure and the flow conditions. However, further research work will be necessary to identify the dispersion coefficients of the two-layer model as a function of the chosen layer structure.

ACKNOWLEDGEMENT

This work was financially supported by the Deutsche Forschungsgemeinschaft within the Forschergruppe "Modellierung des großräumigen Wärme- und Schadstofftransports im Grundwasser"

REFERENCES

Gelhar, L. W. and Axness, C. L. 1983. Three-dimensional Stochastic Analysis of Macrodispersion in Aquifers, Water Resources Res. 19 (1), pp. 161-180.

Kobus, H. 1987. Modellierung des großräumigen Wärme- und Schadstofftransports im Grundwasser, Tätigkeitsbericht 1986/87, Mitteilungen des Instituts für Wasserbau, Heft 66, Universität Stuttgart.

Herr, M., Schäfer, G. and Spitz, K.-H. 1988. Experimental Studies of Mass Transport in Porous Media with Local Heterogeneities, will appear in Journal of Contaminant Hydrology.

Herr, M. 1985. Grundlagen der hydraulischen Sanierung verunreinigter Porengrundwasserleiter, Mitteilungen des Instituts für Wasserbau, Universität Stuttgart, Heft 63.

Mercado, A. 1967. The Spreading Pattern of Injected Waters in a Permeable Stratified Aquifer, Symp. of Haifa, Artificial Recharge and Management of Aquifers, IAHS Pub. 72, pp. 23-26.

Pfannkuch, H.O. 1963. Contribution a l'etude des deplacements de fluides miscibles dans un millieu poreux, Rev. Inst. Fr. Petrol, 18(2), pp. 215-270.

Schäfer, G. 1987. Experimentelle Untersuchungen zum Stofftransport in einem inhomogenen Modellaquifer, Wiss. Bericht HWV 084, Institut für Wasserbau, Universität Stuttgart.

Shamir, U. Y. and Harleman, D. R. F. 1966. Numerical and Analytical Solutions of Dispersion Problems in Homogeneous and Layered Aquifers, Hydrodynamics Laboratory Report No. 89, MIT.

Skopp, J.; Gardner, W. R. and Tyler, E. J. 1981. Solute Movement in Structured Soils: Two-Region Model with Small Interaction, Soil Sci. Soc. Am. J., Vol. 45, pp. 837-842.

Spitz, K.-H. 1985. Dispersion in porösen Medien: Einfluß von Inhomogenitäten und Dichteunterschieden, Mitteilungen des Instituts für Wasserbau, Heft 60, Universität Stuttgart.